Hindawi
Geofluids
Volume 2022, Article ID 9965046, 9 pages
https://doi.org/10.1155/2022/9965046

Research Article

Combination of Methyl from Methane Early Cracking: A Possible Mechanism for Carbon Isotopic Reversal of Overmature Natural Gas

Jingkui Mi,[1,2] **Kun He**,[1,2] **Yanhuan Shuai**,[1,2] **and Jinhao Guo**[1,2]

[1]*State Key Laboratory for Enhanced Oil Recovery, Beijing 100083, China*
[2]*Research Institute of Petroleum Exploration and Development, PetroChina, China*

Correspondence should be addressed to Jingkui Mi; jkmi@petrochina.com.cn

Received 1 April 2021; Accepted 27 October 2021; Published 10 January 2022

Academic Editor: Yunpeng Wang

In this study, a methane (CH_4) cracking experiment in the temperature range of 425–800°C is presented. The experimental result shows that there are some alkane and alkene generation during CH_4 cracking, in addition to hydrogen (H_2). Moreover, the hydrocarbon gas displays carbon isotopic reversal ($\delta^{13}C_1 > \delta^{13}C_2$) below 700°C, while solid carbon appears on the inner wall of the gold tube above 700°C. The variation in experimental products (including gas and solid carbon) with increasing temperature suggests that CH_4 does not crack into carbon and H_2 directly during its cracking, but first cracks into methyl ($CH_3^{\cdot}$) and proton (H^+) groups. $CH_3^{\cdot}$ shares depleted ^{13}C for preferential bond cleavage in ^{12}C–H rather than ^{13}C–H. $CH_3^{\cdot}$ combination leads to depletion of ^{13}C in heavy gas and further causes the carbon isotopic reversal ($\delta^{13}C_1 > \delta^{13}C_2$) of hydrocarbon gas. Geological analysis of the experimental data indicates that the amount of heavy gas formed by the combination of $CH_3^{\cdot}$ from CH_4 early cracking and with depleted ^{13}C is so little that can be masked by the bulk heavy gas from organic matter (OM) and with enriched ^{13}C at $R_o < 2.5\%$. Thus, natural gas shows normal isotope distribution ($\delta^{13}C_1 < \delta^{13}C_2$) in this maturity stage. $CH_3^{\cdot}$ combination (or CH_4 polymerization) intensifies on exhaustion gas generation from OM in the maturity range of $R_o > 2.5\%$. Therefore, the carbon isotopic reversal of natural gas appears at the overmature stage. CH_4 polymerization is a possible mechanism for carbon isotopic reversal of overmature natural gas. The experimental results indicate that although CH_4 might have start cracking at $R_o > 2.5\%$, but it cracks substantially above 6.0% R_o in actual geological settings.

1. Introduction

The notable development in natural gas exploration in the 21st century is the significant discovery of shale gas. Furthermore, some new geochemical and geological characteristics of shale gas have been encountered during exploration, such as the isotopic rollover and/or isotopic reversal of shale gas at very high thermal maturity levels. These features have also been observed in coal-derived tight gas [1–3]. In recent years, substantial research has been conducted to unravel the mechanism of isotopic rollover and reversal of overmature natural gas. However, the question is still not fully understood. Some researchers have suggested that the isotopic reversal of shale gas at overmature stages is caused by mixing of primary gas from kerogen cracking and secondary gas from the cracking of remained hydrocarbons [4–6], while others proposed that the redox reactions between water and CH_4 at 250-300°C generate isotopically light carbon dioxide and hydrogen in the overmature phase, which further interacts to form isotopically light ethane (C_2H_6) and finally causes the isotopic reversal of shale gas [7, 8].

Based on oil-prone kerogen pyrolysis experiments under hydrous and anhydrous conditions, Gao et al. [9] and Sun et al. [10] illustrated that mixing between primary and cracking gases could not yield isotopic reversal, only isotopic rollover. Therefore, the mixing mechanism for isotopic reversal is not experimentally supported. Xia et al. [6] proposed that the mixing between two gas samples with organic

origin can lead to carbon isotopic reversal. However, one end member involved in the mixing model is very dry gas and another is very wet gas. Generally, this phenomenon of the mixing of very dry gas and wet gas does not cooccur in shale system, especially in one with a higher maturity than 2.5% R_o [10]. Thus, mixing cannot be the real mechanism for isotopic reversal of overmature gas. The alternate view on the abnormal isotopic characteristic is impossible in theory. As geological temperature reaches 250–300°C at which CH_4 could react with water, C_2H_6 would react with water prior to CH_4 owing to the comparative lower activation energy. The reaction between C_2H_6 and water would cause residual C_2H_6 to bear heavy carbon isotope. Thus, the carbon isotopic reversal could not occur.

Natural gas with the isotopic reversal feature was originally considered to be of abiogenic origin before shale gas with such feature was found. The abnormal isotopic feature of abiogenic gas was thought to be caused by polymerization (or combination) of CH_4 formed by Fischer–Tropsch synthesis between H_2 and CO_2 (or CO) ([11–13]. Zeng et al. [3] proposed that the carbon isotopic reversal for the deep layer natural gas developed in the Xujiaweizi fault depression, in the Songliao Basin, China, was attributed to the polymerization of CH_4 originating from overmature coal formation source rock. However, the theoretical view of CH_4 polymerization causing the isotopic reversal for abiotic gas or organic gas has not been proven experimentally. Nevertheless, as the direct synthesis of higher hydrocarbons by using CH_4 and metallic catalysts is possible in modern petrochemical industry [9, 14, 15]), the natural formation of heavy hydrocarbon gas by CH_4 polymerization may also be possible. Cheng et al. [16] proved that heavy hydrocarbon gases could generate in isothermal cracking experiments of CH_4, CH_4+Ni, and CH_4+shale conducted in gold tube at 450–580°C. Moreover, three gaseous products in the fifteen groups of CH_4 cracking experiments at different temperature showed isotopic reversal phenomenon.

Therefore, it is important to prove in lab whether CH_4 polymerization can form heavy hydrocarbon gas depleted in $\delta^{13}C$, and it is necessary to determine the geological conditions under which CH_4 polymerization occurs. In this study, a cracking experiment of mixed gas of CH_4 and N_2 is presented. The result shows that several hydrocarbon gaseous components and H_2 are generated. Moreover, the hydrocarbon gases show carbon isotopic reversal before substantial CH_4 cracking. Therefore, we suggest that the combination of methyl from CH_4 early cracking is a possible mechanism for carbon isotopic reversal in overmature natural gas.

2. Sample and Experiment

2.1. Sample. To quantify the content of CH_4 in products at different temperatures, N_2 reference gas was mixed with CH_4. N_2 was selected as reference gas in this experiment as it is the most stable diatomic molecule with a decomposition temperature more than 3000°C. Therefore, it could not crack at the highest temperature used in this experiment (800°C). The gas mixture was purchased from Zhaoge Gas Company, Beijing, China, and the CH_4 and N_2 (v/v) mixing ratio was 89.67% and 10.33%. The carbon isotopic value of CH_4 was -26.07‰, and no other hydrocarbon components were detected in the gas mixture by gas chromatography (GC).

2.2. Experiment. The experiments were performed in a gold tube with a length, outer diameter, and thickness of 100, 5.5, and 0.25 mm, respectively. Prior to loading the gas mixture, one end of the tube was sealed by argon-arc welding. To load gas into the gold tube, a special device was developed to connect a vacuum pump and the open tube mouth. In a typical gas loading procedure, the air in the tube was first removed by the vacuum pump to a pressure less than 2 kPa. Then, the open mouth of the tube was closed by a pincer after the mixing gas was injected into the tube from a gas cylinder. Finally, the open end of tube was sealed by argon-arc welding while the tube was immersed in ice water. The pressure of gas injected in the tube was approximately 4 atm in this experiment, which was monitored via a pressure gauge on the gas cylinder. The exact mass of gas sealed in the tube was accurately calculated by subtracting the mass of the tube before gas loading (Table 1).

The gold tube loaded with gas was put into reactor autoclave, and the temperature was controlled by a computer. Each reactor had an independent temperature controller, and all reactors were kept at a constant pressure of 50 MPa during the course of the experiment. Experimental temperature was programmed as follows: the tube was first heated from 20°C to 300°C in 1 h and held for 30 min and then heated at a heating rate of 20°C/h to the target temperature. After the target temperature was reached, the autoclave heating was stopped, and tubes were moved for analysis at room temperature.

Duplicate gold tubes were used at every temperature point in case of breakage. Moreover, additional tubes were also used as replicates for gas analysis and quantification.

Identification and quantification of individual hydrocarbon and nonhydrocarbon gas components were carried out using a two-channel Wasson-Agilent 7890 series gas chromatograph. The heating program for the GC oven heated from room temperature to 68°C (held isothermal for 7 min), then to 90°C (at a rate of 10°C/min and then held isothermal for 1.5 min.), and finally to 175°C (at a rate of 15°C/min and then held isothermal for 1.5 min). An external standard was used for the chromatographic calibration. Certified gas standards were prepared at a precision of better than ±0.1 mol% for each component made by BAPB Inc., United States.

The stable carbon isotopes of the hydrocarbon gases were determined by using an Isochrom II GC-IRMS coupled with a Poraplot Q column with helium as the carrier gas. The heating started from an initial temperature at 30°C (isothermal for 3 min) with heating at 15°C/min to 150°C and held isothermal for 8 min. The measurement of $\delta^{13}C_1$ was relatively easy, and 8–10 μl gaseous products were enough for the $\delta^{13}C_1$ measurement as a high concentration of CH_4 was present in all gaseous products. To guarantee the accuracy of $\delta^{13}C_2$, more than 400 μl of gas was injected to the inlet of GC-IRMS to maintain the height of the $\delta^{13}C_2$ peak

Table 1: Mass of mixture gas sealed in tube for different temperature experiments.

Temperature (°C)	Weight (mg)		
	Tube	Tube+gas	Sealed gas
425	8135.6	8140.1	4.5
450	8031.3	8035.8	4.5
475	8346.2	8350.6	4.4
500	8546.8	8551.3	4.5
525	8327.1	8331.6	4.5
550	8491.3	8496.0	4.7
575	8328.0	8332.4	4.4
600	8348.4	8352.9	4.5
625	8465.4	8469.9	4.5
650	8312.4	8317.0	4.6
675	8657.4	8661.6	4.2
700	8340.9	8345.2	4.3
725	8973.5	8977.9	4.4
750	8368.1	8372.6	4.5
775	7990.3	7994.6	4.3
800	8684.3	8688.4	4.1

more than half of the reference peak (flat peak in the left of Figure 1) for the low C_2H_6 content in gaseous products. If the height of the $\delta^{13}C_2$ peak was less than half of the reference height, the value of $\delta^{13}C_2$ might have been inaccurate and was thus discarded. The measurement of $\delta^{13}C$ for each component was repeated at least twice to ensure that the error of each component was less than 0.3‰. The $\delta^{13}C$ values for each component presented in this work were the average value of two measurements. Trace carbon isotopes of other hydrocarbon gases were not measured in this study.

3. Experimental Results

3.1. Gas Components. The gaseous products of CH_4 cracking experiments at different temperatures are summarized in Table 2. Besides the original components (CH_4 and N_2) in gaseous products, heavy hydrocarbon gases (including alkane and alkene) and H_2 were generated during the experiment at different temperatures. The CH_4 content clearly decreased with increasing temperature (Figure 2(a)). The CH_4 content decreased by only 1.26% at 700°C, reducing further by 4.91% from 725 to 800°C. Responding to the reduction in CH_4 content, N_2 content increased slightly (0.43%) at 700°C; however, it increased by 4.77% from 725 to 800°C. The percentages of C_2H_6 and H_2 were high in newly formed components and in the same order of magnitude ($\times 10^{-1}$). The content of C_3H_8 was second highest ($\times 10^{-2}$). Other hydrocarbon gases were only presented in trace amounts ($\times 10^{-3}$). The content of all heavy gases increased initially and then decreased with increasing temperature (Figures 2(b) and 2(c)). The corresponding temperatures at which the contents of C_2H_6 and other heavy gas components reached their maximums were 750 and 675°C, respectively. The highest content of total heavy gas was 1.05% at 750°C. The content of total heavy gas decreased to 0.73% at the highest experimental temperature of 800°C. H_2 was detectable only above 500°C, and its content increased with increasing temperature (Figure 2(b)).

3.2. Carbon Isotopes of Gases. As presented in Table 2, $\delta^{13}C_1$ and $\delta^{13}C_2$ generally increased with increasing temperature (Figure 3). The variation of $\delta^{13}C_1$ was not observable within the analytic error (±0.3‰) below 700°C. The value of $\delta^{13}C_1$ clearly increased above 700°C, with an increase of 1.23‰ from 700 to 800°C. The variation in $\delta^{13}C_2$ with increasing temperature could be divided into three segments, gradual increase in $\delta^{13}C_2$ below 625°C, rapid increase from 650 to 725°C, and slow increase above 725°C. The distribution between $\delta^{13}C_1$ and $\delta^{13}C_2$ showed a distinct reversal trend ($\delta^{13}C_1 > \delta^{13}C_2$) for below 725°C and a normal one ($\delta^{13}C_1 < \delta^{13}C_2$) above 725°C.

3.3. Solid Products. The inner walls of the tubes heated to different temperatures are showed in Figure 4. Some black solid can be observed on the inner walls of the tubes above 725°C and was identified as carbon via energy spectrum analysis (Figure 5). The mass of the solid carbon was calculated by subtracting the mass of the tube before gas loading (one end being already welded) from the mass after gas analysis. Although solid carbon could be observed at the inner wall of tubes heated to more than 700°C, the mass could only be measured after heating at 775 and 800°C, using an analytical balance with a measurement error of 0.1 mg, with a mass of 0.2 mg and 0.4 mg, respectively.

4. Discussion

4.1. Heavy Hydrocarbon Gas Generation. The synthesis of heavier hydrocarbons by using CH_4 and metallic catalysts is a popular method in the modern petrochemical industry [9, 14, 15]. Chen et al. [16] reported that heavy hydrocarbon gas could be generated in CH_4 cracking experiments. The overall reaction through thermal coupling or polymerization of CH_4 is generally believed to involve the following stepwise dehydrogenation at high temperatures [17].

$$\begin{array}{ccccccccc} 2CH_4 & \longrightarrow & C_2H_6 & \longrightarrow & C_2H_4 & \longrightarrow & C_2H_2 & \longrightarrow & 2C \\ & & \downarrow & & \downarrow & & \downarrow & & \downarrow \\ & & +H_2 & & +H_2 & & +H_2 & & +H_2 \end{array} \quad (1)$$

In recent years, many researchers have proposed that the CH_4 cracking and formation of higher carbon number hydrocarbons follows a free radical reaction mechanism [16, 18, 19]. The total radical reaction paths are summarized as follows:

$$CH_4 \rightleftharpoons CH\cdot + H\cdot \quad (2)$$

$$2CH_3\cdot \rightleftharpoons C_2H_6 \quad (3)$$

$$C_2H_6 \rightleftharpoons C_2H_5\cdot + H\cdot \quad (4)$$

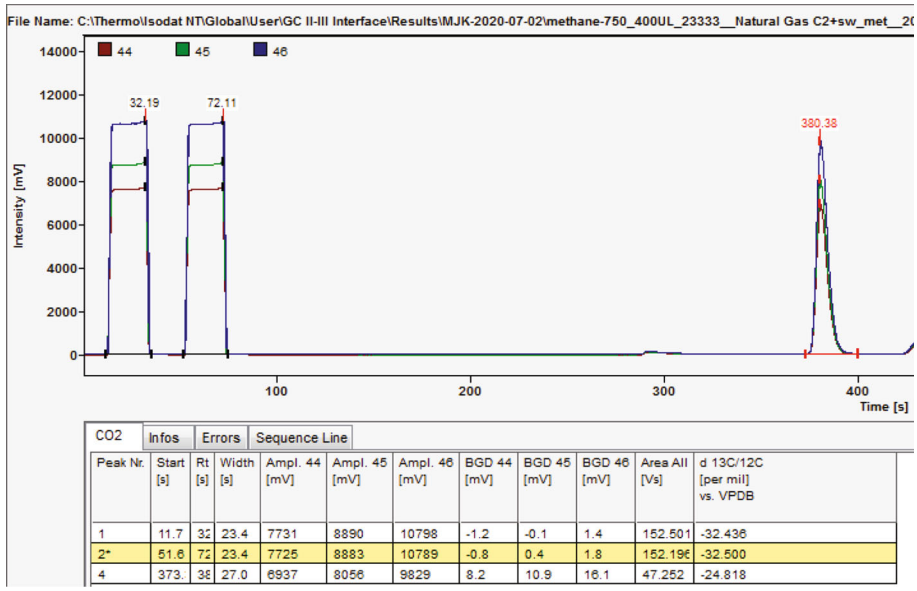

Figure 1: Comparison of carbon isotope peaks between reference and C_2H_6 (750°C).

Table 2: Components and carbon isotopes of gaseous products at different temperatures.

Temperature (°C)	Contents (%)									$\delta^{13}C$ (‰)	
	CH_4	C_2H_6 ($\times10^{-1}$)	C_2H_4 ($\times10^{-3}$)	C_3H_8 ($\times10^{-2}$)	C_3H_6 ($\times10^{-3}$)	iC_4H_{10} ($\times10^{-3}$)	nC_4H_{10} ($\times10^{-3}$)	H_2 ($\times10^{-1}$)	N_2	CH_4	C_2H_6
425	89.66	0.01	0	0.01	0	0	0	0	10.34	-26.01	/
450	89.65	0.01	0	0.02	0	0	0	0	10.35	-26.08	/
475	89.55	0.01	0	0.03	0	0	0	0	10.45	-25.94	/
500	89.53	0.01	0	0.04	0	0	0	0.01	10.47	-25.71	/
525	89.48	0.01	0	0.04	0	0	0	0.05	10.51	-25.71	-33.78
550	89.44	0.02	0	0.04	0	0	0	0.15	10.54	-25.84	-33.51
575	89.3	0.15	0	0.11	0	0	0	0.21	10.66	-25.74	-33.22
600	89.21	0.39	0	0.20	0	0	0	0.35	10.71	-26.01	-32.74
625	89.12	0.69	0.14	0.37	0.31	0	0.27	0.7	10.74	-25.69	-32.47
650	89.06	1.08	0.19	0.56	0.38	0.24	0.37	1.07	10.72	-25.97	-30.26
675	88.66	3.08	2.33	5.19	2.89	1.68	2.56	2.26	10.75	-25.81	-27.47
700	88.41	4.50	1.14	3.97	0.96	0.97	1.62	3.38	10.76	-25.83	-26.02
725	87.25	10.11	1.05	3.75	0.83	0.90	1.39	5.03	11.25	-25.66	-25.11
750	86.25	9.54	0.86	3.41	0.61	0.67	1.15	7.06	12.00	-25.28	-24.82
775	85.02	8.60	0.58	2.63	0.36	0.45	0.68	8.12	13.28	-25.04	-24.68
800	82.34	7.20	0.22	0.75	0.14	0.24	0.30	9.10	16.02	-24.60	-24.50

/: none detected.

$$C_2H_5\cdot \rightleftharpoons C_2H_5\cdot + H\cdot \quad (5)$$

$$C_2H_5\cdot + CH_3\cdot \rightleftharpoons C_3H_8 \quad (6)$$

$$C_xH_y\cdot + CH_3\cdot \rightleftharpoons C_{x+1}H_{y+3} \quad (7)$$

$$H\cdot + H\cdot \rightleftharpoons H_2 \quad (8)$$

$$C_2H_4 \rightleftharpoons C_2H_2 + H_2 \quad (9)$$

$$C_2H_2 \rightleftharpoons 2C + H_5 \quad (10)$$

All aforementioned analysis indicates that CH_4 does not crack into carbon and H_2 directly during early cracking, but first forms $CH_3^{\cdot}$ radicals and protons, and the $CH_3^{\cdot}$ radicals then combine or polymerize into heavy gas. The heavy gas further dehydrogenates and forms unsaturated heavy gas (alkene gas). The unsaturated heavy gas dehydrogenates at increasing temperatures and forms carbon. The experimental result presented in Table 2 shows that alkane and alkene gases are detected in the gaseous products during experimental CH_4 cracking. Solid carbon is only observed above

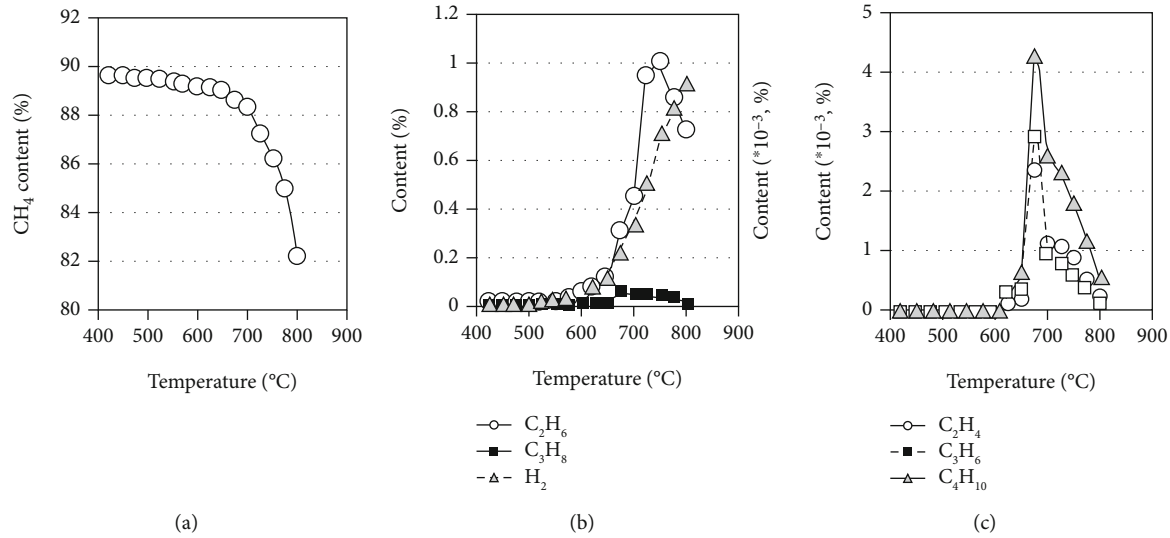

Figure 2: Concentration variation of hydrocarbon gases and H_2 with increasing temperature. (a) Variation in CH_4 content with increasing pyrolysis temperature. (b) Variation in C_2H_6, C_3H_8, and H_2 contents with increasing pyrolysis temperature. (c) Variation in C_2H_4, C_3H_6, and C_4H_{10} contents with increasing pyrolysis.

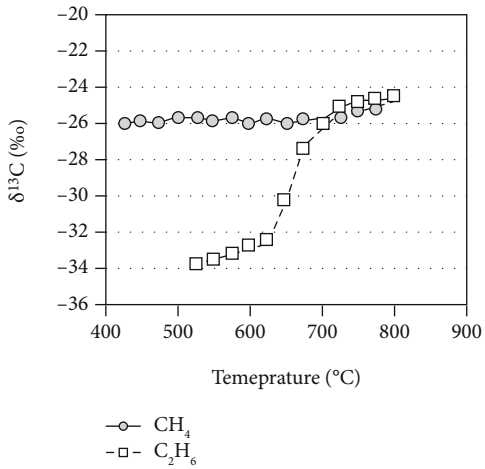

Figure 3: Variation in $\delta^{13}C_1$ and $\delta^{13}C_2$ with increasing temperature.

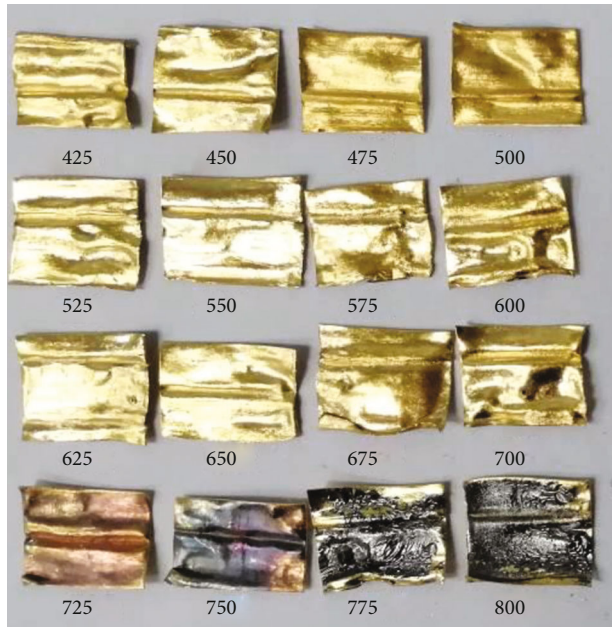

Figure 4: Inner wall photo of a tube heated to different temperatures.

700°C. This indicates that the reaction mechanism of CH_4 cracking experiment is consistent with the aforementioned reaction paths. Although the above reaction might follow a free radical reaction mechanism, the formation of heavy alkane gas during early CH_4 cracking could also be considered as direct CH_4 polymerization. Therefore, isotopic reversal of natural gas owing to CH_4 polymerization is chemically plausible.

The variation of different product components with increasing temperature (Figure 2) could be explained by aforementioned reaction mechanism. Although CH_4 polymerization to form heavy hydrocarbon gas can occur at a relatively low temperature of 425°C, this reaction clearly increases at 625°C. The obvious decrease in CH_4 content above 700°C and the appearance of solid carbon on the tube inner wall at 725°C indicate that the substantial cracking of CH_4 begin in temperature range of 700–725°C. However, the content of heavy hydrocarbon gas continuously increases until 750°C. This result appears to conflict with the general knowledge in chemistry that the thermal stability of heavy gases is lower than that of CH_4. Shuai et al. [20] proved by coal pyrolysis experiment in a confined system that the generation and cracking of C_2H_6 could coexist at high temperatures. Our experimental result does not mean that the thermal stability of heavy gases is higher than that of CH_4, only that the ratio of heavy gas formation by CH_4 polymerization is greater than that of heavy gases cracking into solid carbon in temperature range of 700–750°C. No matter how high the pyrolysis temperature or maturity level of a source

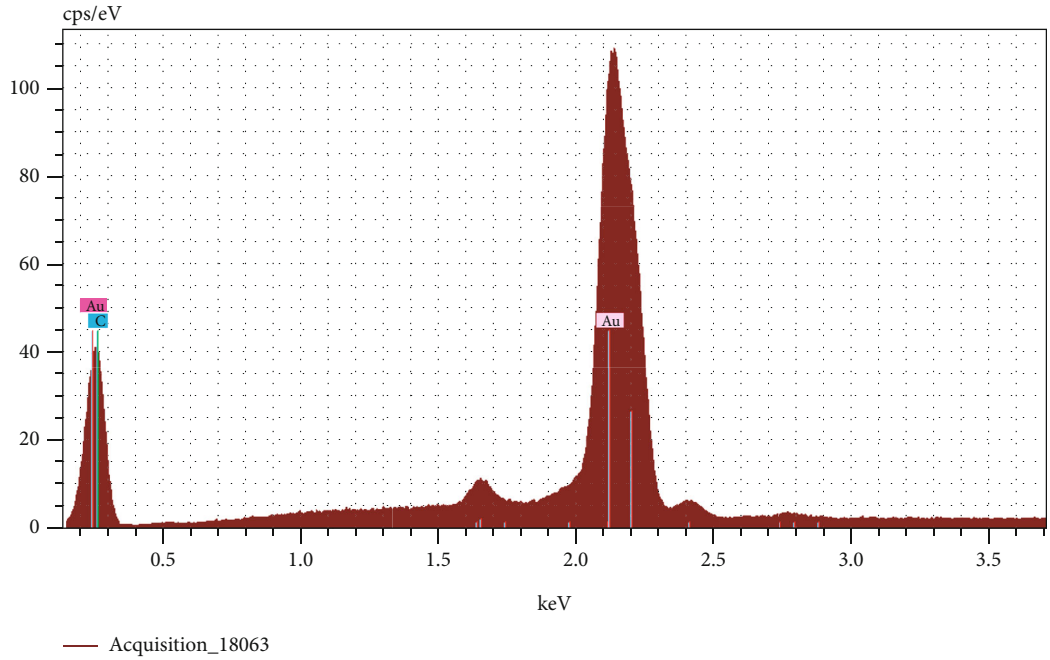

Figure 5: Result of energy spectrum analysis for black solid (775°C).

rock is, there is no gas sample completely without any heavy gas component from in both OM pyrolysis experiments and in natural gas found in sedimentary basins. Some of these heavy gas components could originate from CH_4 polymerization. This is also consistent with the hypothesis proposed by Xia and Gao [19] that heavy gas cracking and generation is a partly reversible reaction at high temperatures. The phenomenon could affect the isotopic composition of C_2H_6 generated in OM pyrolysis experiment in closed system, which becomes more negative at relatively high temperatures (>600°C). Low $\delta^{13}C_2$ values observed may be considered to be erroneous and deleted, as the content of C_2H_6 is very low in gaseous products and the height of $\delta^{13}C_2$ peak is often less than that of the half-height of reference (as in Figure 1). The real reason for the decrease in $\delta^{13}C_2$ in OM pyrolysis experiments in a closed system at high temperatures is the CH_4 polymerization that forms heavy hydrocarbon with a light isotopic composition. The amount of solid carbon generated by heavy gas cracking is so low that the carbon film on the inner wall of tube is very thin and presents a brown to dark brown color at 725 and 750°C (Figure 3), respectively. Above 750°C, the ratio of heavy gas cracking into solid carbon increases, compared to heavy gas generation, and thus, the concentration of heavy gas decreases. The amount of solid carbon increases obviously above 750°C, and the color of tube inner wall darkens.

4.2. Carbon Isotope Fractionation in Heavy Hydrocarbon Gas Generation. Carbon isotope evolution of CH_4 cracking is attributed to kinetic isotope fractionation [16]. The ^{12}C–H and ^{12}C–^{12}C bonds are more chemically active than ^{13}C–H and ^{12}C–^{13}C, respectively [21, 22]. CH_4 undergoes preferential bond cleavage at the ^{12}C–H position rather than ^{13}C–H, leading to the produced $CH_3^{\cdot}$ being depleted in ^{13}C while residual CH_4 is enriched in ^{13}C. When two $CH_3^{\cdot}$ groups combine into C_2H_6, they preferentially form ^{12}C–^{12}C bond, further enhancing depletion in ^{13}C and thus potentially leading to gas isotopic reversal.

Polymerization of CH_4 is the primary reaction in experiment below 700°C. C_2H_6 presents a light carbon isotopic composition, and gas presents a reversal feature (Figure 3). The gradual enrichment of $\delta^{13}C_2$ below 625°C is attributed to weak CH_4 polymerization. The increase in polymerization of CH_4 above 625°C causes rapid enrichment of $\delta^{13}C_2$.

The appearance solid carbon on the tube inner wall at 725°C indicates that the cracking rate is greater than the heavy gas formation rate by CH_4 polymerization in temperature range at 700–725°C. Little cracking of C_2H_6 would cause an obvious enrichment in $\delta^{13}C_2$ in its low concentration (<1.1%). The change in the distribution between $\delta^{13}C_1$ and $\delta^{13}C_2$ from reversal trend to a normal one above 700°C is attributed to C_2H_6 cracking, but not to direct cracking of CH_4 into solid carbon.

4.3. Geological Significance of the Experiment. The ultimate objective of the simulation experiment was to unravel the geological background at which isotopic reversal occurs. To achieve that aim, experimental temperatures must be correlated with actual geological temperatures or maturity (R_o). Mi et al. [23] proposed a method to reconstruct R_o of coal residues generated in a gold tube pyrolysis experiment at the same experimental conditions as our experiment. The relationship between R_o and the experiment temperature in experiment at a heating rate of 20°C/h in the gold tube system is described by

$$R_o = 0.114 \times \exp \cdot (0.00563 \times T) + 0.056, \quad (11)$$

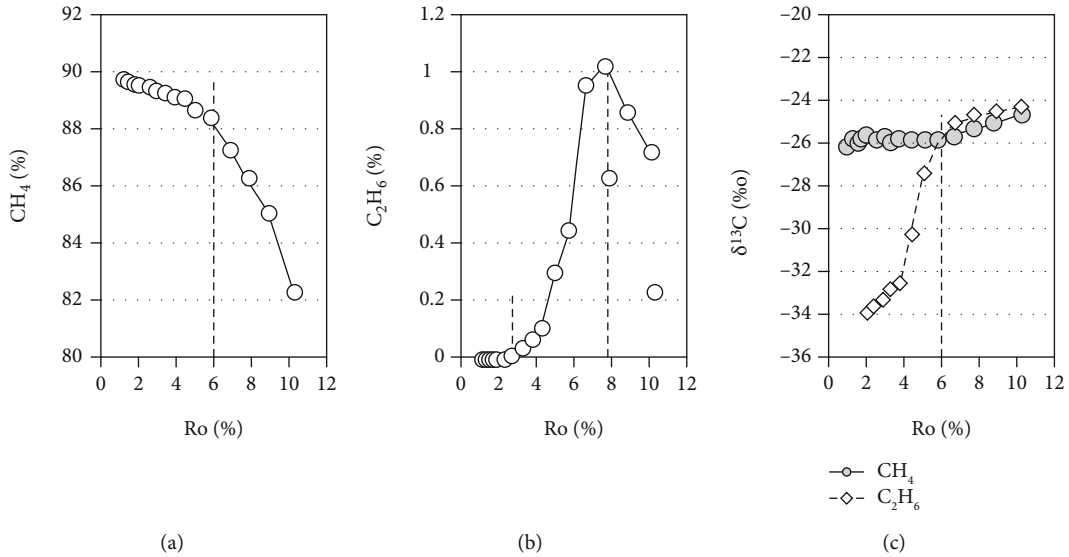

FIGURE 6: Variations in main alkane gas content and $\delta^{13}C_1$ and $\delta^{13}C_2$ with increasing calculated $\%R_o$. (a) Variation in CH_4 content with increasing calculated $\%R_o$. (b) Variation in C_2H_6 content with increasing calculated $\%R_o$. (c) Variation in $\delta^{13}C_1$ and $\delta^{13}C_2$ with increasing calculated $\%R_o$.

$$(T, \text{experiment temperature}/^{\circ}\text{C}). \quad (12)$$

Figure 6 shows the variations in CH_4 content, C_2H_6 content, $\delta^{13}C_1$, and $\delta^{13}C_2$ with increasing R_o calculated by Equation (11). Natural gas exploration has proven that both shale gas and coal formation tight gas with carbon isotopic reversal features are often found in areas where the source rock maturity is more than 2.5–3.0% R_o [1, 2, 4, 8]. This is in good agreement with our experimental result (Figure 6(c)). Although CH_4 polymerization might have started at the relatively low maturity of $R_o = 1.25\%$ (425°C), CH_4 polymerization is slight and only trace heavy gas forms (Figure 5(b)). However, OM has an intense hydrocarbon gas generation potential at this maturity stage. The trace heavy gas produced by CH_4 polymerization with depleted $\delta^{13}C$ would be masked completely by bulk heavy gas from OM enriched in $\delta^{13}C$. Thus, the natural gas presents normal carbon isotopic distribution. The obvious increase in C_2H_6 content indicates that CH_4 polymerization intensified at $R_o = 2.53\%$ (550°C, Figure 6(b)). The gas generation potential from oil-prone OM (type I and II) weakens, and the gas from OM is very dry above 2.5% R_o [24, 25]. Therefore, the heavy gas from CH_4 polymerization with depleted in $\delta^{13}C$ makes the $\delta^{13}C$ value of heavy gas low and displays isotopic reversal of natural gas. Although some gas generation potential exists for type III OM or coal, the gas from this type of OM is very dry with a higher maturity of 2.5% R_o. The trace ethane depleted in $\delta^{13}C$ by CH_4 polymerization leads to carbon isotopic reversal of coal formation tight gas. This was proved by an mixing experiment of two end member natural gases, one is the gas with carbon isotopic reversal and another is coal-derived gas with high dryness and normal carbon isotopic distribution [26]. Although CH_4 polymerization might be an important mechanism of carbon isotopic reversal for natural gas in the maturity range of 2.5–6.0% R_o, it cannot cause the apparent decrease in natural gas resources as only little CH_4 experiences early cracking (or polymerization) in this maturity range. The experiment result shows that the maturity limit for CH_4 bulk cracking in a geological setting is approximately 6.0% R_o (700–725°C). Therefore, the theoretical maturity limit for natural gas exploration should be 6.0% R_o. However, the reported maximum maturity level for shale gas exploration is only 4.0% R_o (in Fayetteville gas field, United States) [4] at present, which is much lower than the maturity of 6.0% R_o. The upper maturity limit for gas exploration is also controlled by other geological and chemical factors (such as potential and rate of gas generation, gas diffusion rate, preserved condition, and shale catalysis for methane cracking). As the upper maturity limit of gas generation for oil-prone OM is 3.5% R_o [24], therefore, it is acceptable in theory to explore natural gas exploration in marine shale with maturity levels in 3.5–6.0% R_o. However, we suggest to not lightly practice natural gas exploration in oil-prone shale with the maturity space of 3.5–6.0% R_o as the tiny CH_4 molecule stored in shale is easily lost to exhaustion without the generated gas supply from shale in very long geological history.

5. Conclusion

Our experimental result shows that heavy hydrocarbon gases (including alkanes and alkenes) are generated during CH_4 cracking, in addition to H_2. Moreover, the heavy gas displays the feature of depleted carbon isotope composition in the early stage of CH_4 cracking. CH_4 does not crack into carbon and H_2 directly, but first into $CH_3^{\cdot}$ and H^+ during early cracking. CH_4 undergoes preferential bond cleavage of ^{12}C–H rather than ^{13}C–H owing to the relatively higher chemical activity of ^{12}C–H compared with that of ^{13}C–H. The produced $CH_3^{\cdot}$ is depleted in ^{13}C, and thus, C_2H_6 formed by $CH_3^{\cdot}$ combination (or CH_4 polymerization) is also depleted in ^{13}C. CH_4 polymerization at the relatively

low maturity stage of $R_o < 2.5\%$ is so weak that the trace heavy gas by CH_4 polymerization with depleted ^{13}C can be masked by bulk heavy gas with enriched ^{13}C from OM. Natural gas generated in this maturity range would exhibit a normal trend of carbon isotopic distribution. Relatively intense CH_4 polymerization accompanied with the weak gas generation from OM causes carbon isotopic reversal appear in natural gas beyond R_o of 2.5%. CH_4 polymerization is a possible mechanism for carbon isotopic reversals of overmature natural gas. The maturity threshold for substantial CH_4 cracking under actual geological settings is approximately 6.0% R_o.

Data Availability

The data in paper titled "Combination of methyl from methane early cracking: a possible mechanism for carbon isotopic reversal of overmature natural gas" is the result of relative experiment involved in this study. All the data is in the paper. There is no restriction on data access and reader could get easily.

Additional Points

Highlights. (1) Heavy hydrocarbon gas is generated and bears depleted $\delta^{13}C$ during CH_4 early cracking. (2) CH_4 does not crack directly into carbon and H_2, but first forms $CH_3^{\cdot}$ and H^+ groups during early cracking. (3) The $CH_3^{\cdot}$ shares depleted ^{13}C owing to preferential bond cleavage of ^{12}C–H rather than ^{13}C–H. (4) The $CH_3^{\cdot}$ combination leads to depleted $^{13}C_2$ and causes isotopic reversal for overmature natural gas. (5) The threshold of substantial CH_4 cracking is 6.0% R_o under actual geological settings.

Conflicts of Interest

The authors declare that they have no conflicts of interest.

Acknowledgments

This research is supported by the State Key Program of National Natural Science of China (Grant No. 42030804) and the National Natural Science Foundation of China (Grant No. 41673047). I would like to thank Doctor Keyu Liu for polishing our manuscript.

References

[1] J. X. Dai, Y. Y. Ni, S. P. Huang et al., "Secondary origin of negative carbon isotopic series in natural gas," *Journal of Natural Gas Geoscience*, vol. 1, no. 1, pp. 1–7, 2016.

[2] Z. Q. Feng, D. Liu, S. P. Huang, D. Y. Gong, and W. L. Peng, "Geochemical characteristics and genesis of natural gas in the Yan'an gas field, Ordos Basin, China," *Organic Geochemistry*, vol. 102, pp. 67–76, 2016.

[3] H. S. Zeng, J. K. Li, and Q. L. Huo, "A review of alkane gas geochemistry in the Xujiaweizi fault-depression, Songliao Basin," *Marine and Petroleum Geology*, vol. 43, pp. 284–296, 2013.

[4] F. Hao and H. Y. Zou, "Cause of shale gas geochemical anomalies and mechanisms for gas enrichment and depletion in high-maturity shales," *Marine and Petroleum Geology*, vol. 44, pp. 1–12, 2013.

[5] B. J. Tilley and K. Muehlenbachs, "Isotope reversals and universal stages and trends of gas maturation in sealed, self-contained petroleum systems," *Chemical Geology*, vol. 339, pp. 194–204, 2013.

[6] X. Y. Xia, J. Chen, R. Braun, and Y. C. Tang, "Isotopic reversals with respect to maturity trends due to mixing of primary and secondary products in source rocks," *Chemical Geology*, vol. 339, pp. 205–212, 2013.

[7] R. C. Burruss and C. D. Laughrey, "Carbon and hydrogen isotopic reversals in deep basin gas: evidence for limits to the stability of hydrocarbons," *Organic Geochemistry*, vol. 41, no. 12, pp. 1285–1296, 2010.

[8] J. Zumberge, K. J. Ferworn, and S. Brown, "Isotopic reversal ('rollover') in shale gases produced from the Mississippian Barnett and Fayetteville formations," *Marine and Petroleum Geology*, vol. 31, no. 1, pp. 43–52, 2012.

[9] L. Gao, A. Schimmelmann, Y. C. Tang, and M. Mastalerz, "Isotope rollover in shale gas observed in laboratory pyrolysis experiments: insight to the role of water in thermogenesis of mature gas," *Organic Geochemistry*, vol. 68, pp. 95–106, 2014.

[10] M. M. Sun, J. K. Mi, Z. H. Feng, X. Q. Li, and J. H. Zhang, "The feature comparison of hydrocarbon generation forItype of organic matter in gold tube using two kind of heating methods (in Chinese with English abstract)," *Nat. Gas Geo.*, vol. 26, pp. 1156–1164, 2015.

[11] J. Horita and M. E. Berndt, "Abiogenic $_{\text{Methane}}$ formation and isotopic fractionation under hydrothermal conditions," *Science*, vol. 285, no. 5430, pp. 1055–1057, 1999.

[12] G. X. Hu, Z. Y. Quyang, X. Wang, and Q. B. Wen, "Carbon isotopic fractionation in the process of Fischer-Tropsch reaction in primitive solar nebula," *Science in China Series D: Earth Sciences*, vol. 41, no. 2, pp. 202–207, 1998.

[13] B. Sherwood Lollar, G. Lacrampe-Couloume, K. Voglesonger, T. C. Onstott, L. M. Pratt, and G. F. Slater, "Isotopic signatures of CH_4 and higher hydrocarbon gases from Precambrian Shield sites: a model for abiogenic polymerization of hydrocarbons," *Geochimica et Cosmochimica Acta*, vol. 72, no. 19, pp. 4778–4795, 2008.

[14] C. Karakaya and R. J. Kee, "Progress in the direct catalytic conversion of methane to fuels and chemicals," *Progress in Energy and Combustion Science*, vol. 55, pp. 60–97, 2016.

[15] D. C. Upham, V. Agarwal, A. Khechfe et al., "Catalytic molten metals for the direct conversion of methane to hydrogen and separable carbon," *Science*, vol. 358, no. 6365, pp. 917–921, 2017.

[16] B. Chen, J. B. Xu, Q. Deng et al., "Methane cracking within shale rocks: a new explanation for carbon isotope reversal of shale gas," *Marine and Petroleum Geology*, vol. 121, article 104591, 2020.

[17] T. V. Choudhary, E. Aksoylu, and D. W. Goodman, "Nonoxidative activation of methane," *Catalysis Reviews*, vol. 45, no. 1, pp. 151–203, 2003.

[18] C. Karakaya, H. Zhu, C. Loebick, J. G. Weissman, and R. J. Kee, "A detailed reaction mechanism for oxidative coupling of methane over $Mn/Na_2WO_4/SiO_2$ catalyst for non-isothermal conditions," *Catalysis Today*, vol. 312, no. 15, pp. 10–22, 2018.

[19] X. Y. Xia and Y. Gao, "Depletion of ^{13}C in residual ethane and propane during thermal decomposition in sedimentary basins," *Organic Geochemistry*, vol. 125, pp. 121–128, 2018.

[20] Y. H. Shuai, P. A. Peng, Y. R. Zou, and S. C. Zhang, "Kinetic modeling of individual gaseous component formed from coal in a confined system," *Organic Geochemistry*, vol. 37, no. 8, pp. 932–943, 2006.

[21] F. Lorant, A. Prinzhofer, F. Behar, and A. Y. Huc, "Carbon isotopic and molecular constraints on the formation and the expulsion of thermogenic hydrocarbon gases," *Chemical Geology*, vol. 147, no. 3-4, pp. 249–264, 1998.

[22] Y. Tang, J. K. Perry, P. D. Jenden, and M. Schoell, "Mathematical modeling of stable carbon isotope ratios in natural gases†," *Geochimica et Cosmochimica Acta*, vol. 64, no. 15, pp. 2673–2687, 2000.

[23] J. K. Mi, K. He, J. J. Fan, G. Y. Hu, and B. Zhang, "Thermal maturity determination for oil prone organic matter based on the Raman spectra of artificial matured samples," *Vibrational Spectroscopy*, vol. 104, article 102940, 2019.

[24] J. K. Mi, S. C. Zhang, J. Su et al., "The upper thermal maturity limit of primary gas generated from marine organic matters," *Marine and Petroleum Geology*, vol. 89, pp. 120–129, 2018.

[25] B. P. Tissot and D. H. Welte, *Petroleum Formation and Occurrence*, Springer-Verlag, Edition 2 edition, 1985.

[26] T. Liu, J. K. Mi, and M. Zhang, "Carbon isotopic reversal numerical simulation of deep-seated gases, Songliao Basin (in Chinese with English abstract)," *Nat. Gas Geo*, vol. 19, no. 5, pp. 722–726, 2008.